articles

molecular pharmaceutics

Reducing the Background Fluorescence in Mice Receiving Fluorophore/Inhibitor DNA Duplexes

Minmin Liang,[†,‡] Xinrong Liu,[†] Guozheng Liu,[†] Shuping Dou,[†] Dengfeng Cheng,[†] Yuxia Liu,[†] Mary Rusckowski,[†] and Donald J. Hnatowich*[,†]

Department of Radiology, University of Massachusetts Medical School, Worcester, Massachusetts 01655, United States, and National Laboratory of Biomacromolecules, Institute of Biophysics, Chinese Academy of Sciences, Beijing 100101, China

Received May 17, 2010; Revised Manuscript Received November 30, 2010; Accepted December 6, 2010

Abstract: In principle, a DNA duplex consisting of an antisense fluorophore-conjugated major strand hybridized to a shorter complementary inhibitor-conjugated minor strand should provide fluorescence only in the tumor after intravenous administration if designed to remain intact except in the presence in tumor of its mRNA target. While we have obtained impressive tumor images in mice using this approach, there remains some background fluorescence. In this study, tissue homogenates of selected mouse organs were incubated with a test duplex and the kinetics of duplex dissociation in normal tissues were measured. In this manner we were able to identify the liver as the likely major source responsible for the duplex dissociation providing this fluorescence background. Thereafter liver homogenates were used to screen a series of duplex candidates with variable-length minor strands, and dissociation was measured by gel electrophoresis. The selected fluorophore/inhibitor duplex with improved stability displayed an insignificant ($P > 0.05$) background fluorescence after administration to SKH-1 normal mice and apparently without affecting target mRNA binding in vitro in cell culture or in vivo in tumor bearing mice.

Keywords: Optical imaging; background fluorescence; fluorophore/inhibitor; DNA duplex

Introduction

Fluorophore-labeled oligomers such as DNA for antisense imaging of messenger RNA (mRNA) are of potential use for the optical imaging of surface cancers and cancers accessible at surgery or by endoscopy.[1−3] However, when administered in this fashion as a fluorophore-conjugated singlet DNA, in addition to autofluorescence, a background is expressed as the DNA accumulates in normal tissues.[4−6] The result can be severely limited target-to-background ratios and decreased detection sensitivity. To address this problem, approaches are under development to increase the accumulation of fluorescence probes in target tissues and to reduce accumulations in normal tissues.[7−15]

* Corresponding author. Mailing address: University of Massachusetts Medical School, Department of Radiology, 55 Lake Avenue North, Worcester, MA 01655. Tel: 774-442-4256. Fax: 508-856-4572. E-mail: Donald.Hnatowich@umassmed.edu.

† University of Massachusetts Medical School.

‡ Chinese Academy of Sciences.

(1) Liu, X.; Wang, Y.; Nakamura, K.; Liu, G.; Dou, S.; Kubo, A.; Rusckowski, M.; Hnatowich, D. J. Optical antisense imaging of tumor with fluorescent DNA duplexes. *Bioconjugate Chem.* **2007**, *18*, 1905–1911.

(2) Liang, M.; Liu, X.; Cheng, D.; Nakamura, K.; Wang, Y.; Dou, S.; Liu, G.; Rusckowski, M.; Hnatowich, D. J. Optical antisense tumor targeting in vivo with an improved fluorescent DNA duplex probe. *Bioconjugate Chem.* **2009**, *20*, 1223–1227.

(3) Lewis, M. R.; Jia, F. Antisense imaging: and miles to go before we sleep. *J. Cell. Biochem.* **2003**, *90*, 464–472.

(4) Ntziachristos, V.; Bremer, C.; Weissleder, R. Fluorescence imaging with near-infrared light: New technological advances that enable in vivo molecular imaging. *Eur. Radiol.* **2003**, *13*, 195–208.

(5) Tarik, F. M.; Sanjiv, S. G. Molecular imaging in living subjects: seeing fundamental biological processes in a new light. *Genes Dev.* **2003**, *17*, 545–580.

(6) Bremer, C.; Weissleder, R. In vivo imaging of gene expression. *Acad. Radiol.* **2001**, *8*, 15–23.

10.1021/mp100229z
Published on Web 12/06/2010

Recognizing that labeled probes to some degree will always accumulate in normal tissues following intravenous administrations, this laboratory is developing an alternative approach that, in principle, will provide fluorescence only in target tissues despite what may be a less-than-favorable biodistribution. We are developing linear fluorophore/inhibitor-conjugated oligomer duplexes for optical fluorescence imaging, at present largely limited to antisense targeting.[1,2,16] Duplexes consisting of a fluorophore-conjugated antisense DNA major strand hybridized to a shorter complementary inhibitor-conjugated DNA minor strand are being designed to remain intact and therefore nonfluorescent in all normal tissue but to dissociate only in the presence of its mRNA target in tumor tissue. Thus, the fluorescence background should in principle be low to nonexistent when compared to conventional optical imaging methods. In previous reports,[1,2] we have shown proof-of-concept that, when administered as this fluorescence-inhibited duplex, dissociation occurs in tumor by an antisense mechanism and that impressive tumor-to-background fluorescence ratios are achievable. However, some background fluorescence persists. To investigate the dissociation of the duplex in normal tissue that must be occurring to explain this background, we used a stability assay consisting of blood plasma and homogenates derived from whole mouse liver and kidney incubated with test duplexes and capable of measuring the kinetics of duplex dissociation. Thereafter gel electrophoresis was used to screen a series of DNA duplex candidates for those with improved stability. Based on the screening results, the selected fluorophore/inhibitor duplex was administered to SKH-1 normal mice for background fluorescence evaluation, and to KB-G2 tumor bearing mice for mRNA targeting.

Materials and Methods

The uniform phosphorothioate (PS) DNA antisense (5′-AAG-ATC-CAT-CCC-GAC-CTC-GCG-CTC-C-3′) major strand against mdr1 mRNA,[1,2] either native (i.e., unlabeled) or conjugated with the Cy5.5 fluorophore on the 3′ end via a three carbon linker, were purchased from Integrated DNA Technologies (Coralville, IA, USA). The unlabeled duplexes were formed by hybridization with a complementary cDNA uniform unlabeled phosphodiester (PO) minor strand with one of five chain lengths, also obtained from integrated DNA Technologies. The fluorophore-conjugated duplexes were formed by hybridization of the Cy5.5 conjugated major strand with a 10 to 22 mer PO DNA minor strand conjugated with a Black Hole Quencher 3 (BHQ-3) inhibitor on the 5′ end attached via a two carbon linker and obtained from Biosearch Technologies (Novato, CA, USA). The 96-well black microplates were obtained from Corning (Wilkes Barre, PA, USA). Proteinase K was purchased from Pierce (Rockford, IL; USA).

The KB-G2 (mdr1++) and KB-31 (mdr1+/−) cell lines are both of human epidermoid carcer origin. The KB-G2 cell line was transfected from its parent KB-31 to increase expression of Pgp. The cell lines were a gift from Isamu Sugawara (Research Institute of Tuberculosis, Tokyo, Japan) and were cultured overnight at 37 °C, 5% CO_2, in Dulbecco's modified Eagle's medium (DMEM, Invitrogen, Carlsbad, CA, USA) containing 10% fetal bovine serum (FBS). Male hairless SKH-1 mice and NIH Swiss nude mice were obtained from Taconic Farms (Germantown, NY, USA). The chlorophyll-free food was from Harlan Teklad (AIN-93G Purified Diet, Madison, WI, USA).

Homogenate and Blood Plasma Preparation. Livers and kidneys were excised from mice and immediately minced in ice-cold phosphate buffered saline solution (PBS), washed twice and homogenized with an addition of 1:3 (wt/vol) ice-cold 100 mM Tris-HCl buffer (pH 8.0) in a tissue homogenizer on ice. Each crude homogenate was then centrifuged at 4 °C for 10 min at 2000*g*, the sediment was discarded, and the supernatant was collected and frozen at −80 °C until required for the subsequent incubations.

Fresh blood was transferred into Vacutainer tubes (Becton Dickinson, Franklin Lakes, NJ, USA) from mice sacrificed under anesthesia. For use in the subsequent incubations, the blood plasma was separated by centrifugation at 2000*g* for 10 min.

Fluorescence Homogenate Assay. The 25 mer PS DNA conjugated with a 3′ Cy5.5 fluorophore was hybridized with the shortest, and therefore presumably the least stable, 5′ BHQ-3 conjugated minor strand. Thus the PS DNA25-Cy5.5/PO cDNA10-BHQ3 duplex was incubated in liver and kidney homogenates, blood plasma, 70% mouse serum, and PBS

(7) Ogawa, M.; Kosaka, N.; Longmire, M. R.; Urano, Y.; Choyke, P. L.; Kobayashi, H. Fluorophore-quencher based activatable targeted optical probes for detecting in vivo cancer metastases. *Mol. Pharmaceutics* **2009**, *6*, 386–95.
(8) Weissleder, R. A clearer vision for in vivo imaging. *Nat. Biotechnol.* **2001**, *19*, 316–317.
(9) Ogawa, M.; Kosaka, N.; Choyke, P. L.; Kobayashi, H. In vivo molecular imaging of cancer with a quenching near-infrared fluorescent probe using conjugates of monoclonal antibodies and indocyanine green. *Cancer Res.* **2009**, *69*, 1268–1272.
(10) Marras, S. A.; Kramer, F. R.; Tyagi, S. Efficiencies of fluorescence resonance energy transfer and contact-mediated quenching in oligonucleotide probes. *Nucleic Acids Res.* **2002**, *30*, e122.
(11) Frangioni, J. V. In vivo near-infrared fluorescence imaging. *Curr. Opin. Chem. Biol.* **2003**, *7*, 626–634.
(12) Jares-Erijman, E.; Jovin, T. FRET imaging. *Nat. Biotechnol.* **2003**, *21*, 1387–1395.
(13) Montet, X.; Ntziachristos, V.; Grimm, J.; Weissleder, R. Tomographic fluorescence mapping of tumor targets. *Cancer Res.* **2005**, *65*, 6330–6336.
(14) Silverman, A. P.; Kool, E. T. Quenched probes for highly specific detection of cellular RNAs. *Trends Biotechnol.* **2005**, *23*, 225–230.
(15) Ogawa, M.; Kosaka, N.; Choyke, P. L. Tumorspecific detection of an optically targeted antibody combined with a quencher-conjugated neutravidin "quencher-chaser": a dual "quench and chase" strategy to improve target to nontarget ratios for molecular imaging of cancer. *Bioconjugate Chem.* **2009**, *20*, 147–154.
(16) Zhang, S.; Liu, G.; Liu, X.; Yin, D.; Dou, S.; He, J.; Rusckowski, M.; Hnatowich, D. J. Initial in vitro and in vivo studies of fluorescence quenching by linear oligomer hybridization. *Bioconjugate Chem.* **2007**, *18*, 1170–1175.

buffer at 100 nM at 37 °C with gentle shaking for various times up to 6 h. After each incubation, proteinase K was added to a final concentration of 0.5 mg/mL and the mixture incubated for another 1 h at 37 °C to eliminate autofluorescence interference from tissue proteins. The final solution was immediately measured for fluorescence in a 96-well microplate on a microplate reader (Safire, Tecan Group Ltd., Switzerland).

Duplex Screening by Electrophoresis. Based on the results of the fluorescence homogenate assay, the further evaluation of duplex stability was performed only in liver homogenates. Five unlabeled DNA duplexes were prepared with the same PS major strand but with different PO minor strand from 10 to 25 mer (i.e., PS25/PO25, PS25/PO22, PS25/PO14 and PS25/PO10). The duplex PS25/PO18 has been investigated previously[1] and was included as a standard of comparison. After incubation at 20 μM in liver homogenate at 37 °C with gentle shaking for up to 20 h, these DNA duplex samples were analyzed on an 8.6 × 6.8 cm 15% polyacrylamide gel (Bio-Rad Laboratories Inc., Hercules, CA, USA) using 1× TBE buffer and visualized by silver staining. Duplex dissociation will result in a less intense or nonexistent band. DNA quantitation of duplex band intensity was performed by the Image J software.[18]

Target Cell Binding Study. The cell binding studies were performed in KB-G2 (mdr1++) and KB-31(mdr1+/−) cells in 96-well plates seeded at 10^4 cells per well and incubated with 10% FBS/DMEM culture medium overnight. The anti mdr1 PS DNA as the duplex PS DNA25-Cy5.5/PO cDNA22-BHQ3 at different concentrations was incubated with KB-G2 and KB-31 cells in 1% FBS/DMEM medium at 37 °C for 3 h. The cells were then washed twice with 1% FBS/DMEM culture medium and twice with PBS, and were lysed before measuring the fluorescence. The lysis buffer[1] was added at 100 μL per well, and the cells were incubated for 1 h at 37 °C. The fluorescence intensity of each lysing solution was measured on the microplate reader.

Animal Studies. All animal studies were performed with the approval of the UMMS Institutional Animal Care and Use Committee. Nude mice were each injected subcutaneously in the left thigh with a 100 μL suspension containing 10^6 KB-G2 cells and were used for imaging when tumors were about 0.7 cm in any dimension. Mice were placed on a chlorophyll-free food for 5 days before imaging. The PS DNA25-Cy5.5/PO cDNA22-BHQ3 duplex was formed by mixing the two single strands at 1:1, 1:10 or 1:50 molar ratio and heating at 95 °C for 5 min to dissociate any intrastrand duplexes before cooling to room temperature. To evaluate the background fluorescence, SKH-1 mice were each administered 1 nmol of PS DNA25-Cy5.5/PO cDNA22-BHQ3 duplex with and without excess inhibitor minor strand in 100 μL of PBS via a tail vein. Additional nude mice were administered the PS DNA25-Cy5.5/PO cDNA22-BHQ3 duplex prepared at a 1:10 molar ratio to evaluate the target mRNA binding in vivo. Fluorescence imaging was performed on an IVIS 100 small-animal imaging system (Xenogen, Alameda, CA, USA) using a Cy5.5 filter set. During imaging, the animals were lightly anesthetized with 1.5% isoflurane in 2 L/min oxygen. Fluorescence images were acquired at various time points using a 0.5 s exposure time (f/stop 4). Images and measurements of fluorescence were acquired and analyzed with Living Image 2.5 software (Xenogen).

Quenching efficiency was calculated by the following equation:

$$[1 - (F_{\text{duplex}} - F_{\text{background}})/(F_{\text{singlet}} - F_{\text{background}})] \times 100\%$$

where F_{duplex} refers to mice receiving the PS DNA25-Cy5.5/PO cDNA22-BHQ3 duplex, $F_{\text{background}}$ refers to mice receiving only PBS, and F_{singlet} refers to mice receiving the PS DNA25-Cy5.5 singlet, in each case as the whole body fluorescence intensity averaged over the three animals. All images were in the dorsal view.

Results

Fluorescence Homogenate Assay. To measure the dissociation of our fluorophore/inhibitor antisense duplex in vivo and to identify the tissue(s) responsible for the fluorescence background, the duplex with the shortened minor strand, PS DNA25-Cy5.5/PO DNA10-BHQ3, was incubated in liver and kidney homogenates at 100 nM and 37 °C with gentle shaking for up to 6 h. Proteinase K at 0.5 mg/mL was then added and the homogenates were incubated for another 1 h at 37 °C to dissociate tissue proteins. The mixture was then added into a 96-well plate, and the fluorescence was measured immediately on the microplate reader. The identical duplex, also at 100 nM, was also incubated in 37 °C 70% fresh mouse serum, blood plasma and PBS in the identical manner. Figure 1 presents the fluorescence intensity of the duplex as a function of incubation time in each medium. As shown, the most pronounced and rapid increase in the fluorescence signal with incubation time was in the liver homogenate. The increase was less pronounced in the kidney homogenate while incubation in plasma, serum or PBS resulted in little to no increase in fluorescence. These results suggest that nonspecific dissociation of the duplex in vivo occurs by some mechanism primarily in liver.

Duplex Screening by Electrophoresis. A series of five unlabeled DNA duplexes at 20 μM were incubated in the liver homogenate at 37 °C with gentle shaking for up to 20 h. The incubated DNA samples were then analyzed by gel electrophoresis with silver staining, and the intensity of the DNA bands was quantified. Figure 2A presents the gel images for the PS25/PO22 duplex (left panel) and PS25/PO18 (right panel). In both cases, the gels show the result of incubating the duplex at 37 °C in saline (lane 1), and in the liver homogenate immediately (lane 2) and after 1 h (lane

(17) Liu, X.; Wang, Y.; Nakamura, K.; Kawauchi, S.; Akalin, A.; Cheng, D.; Chen, L.; Rusckowski, M.; Hnatowich, D. J. Auger radiation-induced, antisense-mediated cytotoxicity of tumor cells using a 3-component streptavidin-delivery nanoparticle with 111In. *J. Nucl. Med.* **2009**, *50*, 582–90.

(18) Collins, J. T. Image J for microscopy. *BioTechniques* **2007**, *43*, S25–S30.

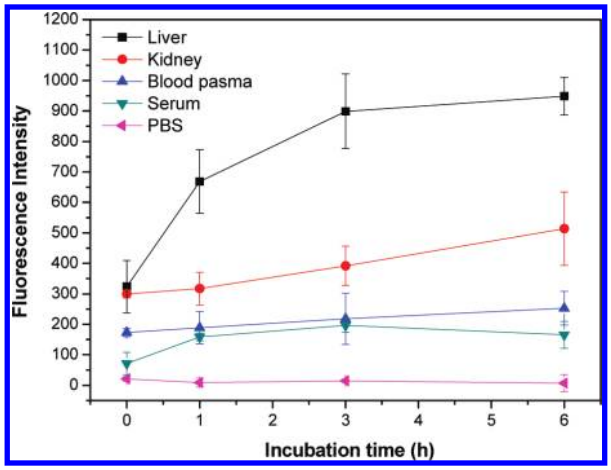

Figure 1. Fluorescence intensity of the PS DNA25-Cy5.5/PO DNA10-BHQ3 duplex after incubation in liver or kidney homogenate, blood plasma, 70% normal mouse serum or PBS over 6 h at 37 °C. Error bars represent standard deviations for three replicates.

3), 3 h (lane 4) and 20 h (lane 5) of incubation. In both cases the duplex band shows evidence of immediate duplex dissociation that continues over time (the remaining bands within each gel are present in the analysis of the homogenate itself). Figure 2B presents the results of quantitating the unlabeled duplex band intensity in the gel images for all five duplexes. As shown, there is no change in band intensity and therefore no duplex dissociation for the PS25/PO25 duplex even after 20 h of incubation while the PS25/PO22 duplex is similarly stable for at least 5 h. By contrast, the remaining duplexes show an immediate and striking dissociation in the first hour that continues slowly thereafter. In the case of both the PS25/PO14 and PS25/PO10 duplexes, the band intensity decreased about 80% after 1 h while this decrease in the case of the PS25/PO18 was about 50%. Since the intended application requires that a minor strand be hybridized with a major strand, the PS25/PO22 duplex was selected for the animal study of fluorescence background evaluation and tumor targeting.

Background Fluorescence Evaluation in Normal Mice. Figure 3 presents the fluorescence of microtubes containing PS DNA25-Cy5.5 singlet in PBS buffer before and after hybridizing with the complementary PO DNA22-BHQ3 singlet at the molar ratios of 1:1, 1:10 and 1:50. The fluorescence intensity is clearly highest for PS DNA25-Cy5.5 singlet and decreased as the molar ratio of PO DNA22-BHQ3 increased. When the singlets were added at a 1:1 molar ratio,

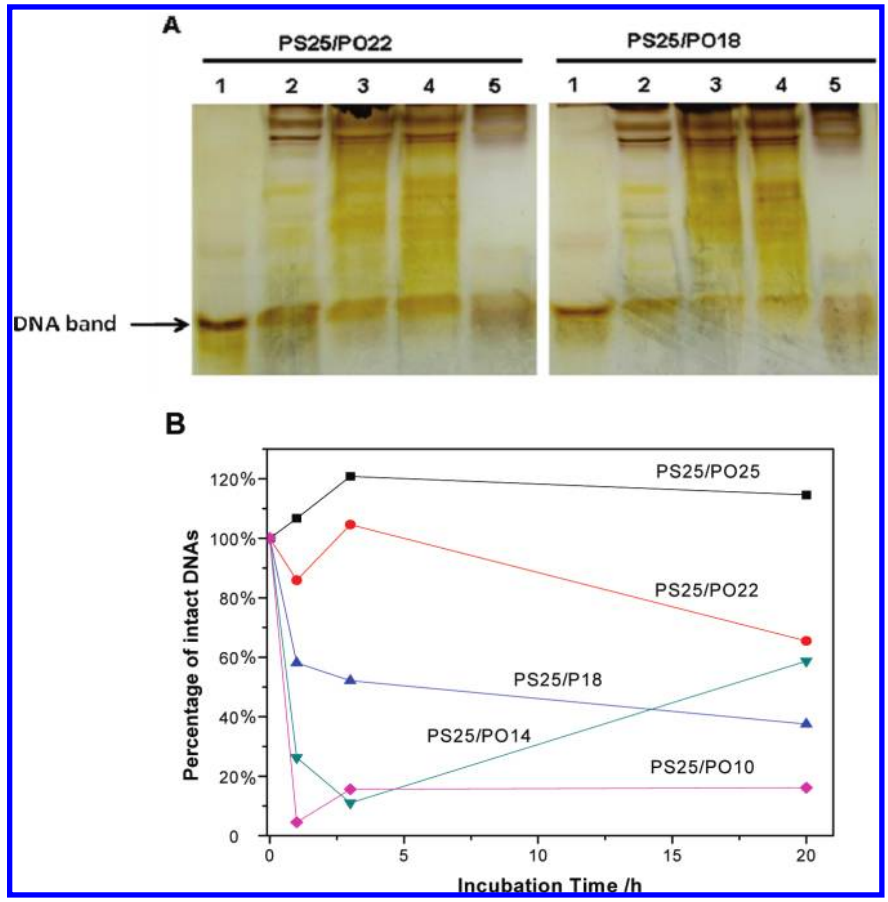

Figure 2. (A) Gel images obtained after incubating the unlabeled PS25/PO22 (left panel) and PS25/PO18 (right panel) duplexes at 37 °C in saline (lane 1), and in liver homogenate immediately (lane 2), after 1 h (lane 3), 3 h (lane 4) and 20 h (lane 5) of incubation. (B) Showing the results of quantitating the DNA band intensity within the gels for the five DNA duplexes as a function of incubation time. Results are presented as the percent of intact duplex set initially at 100%.

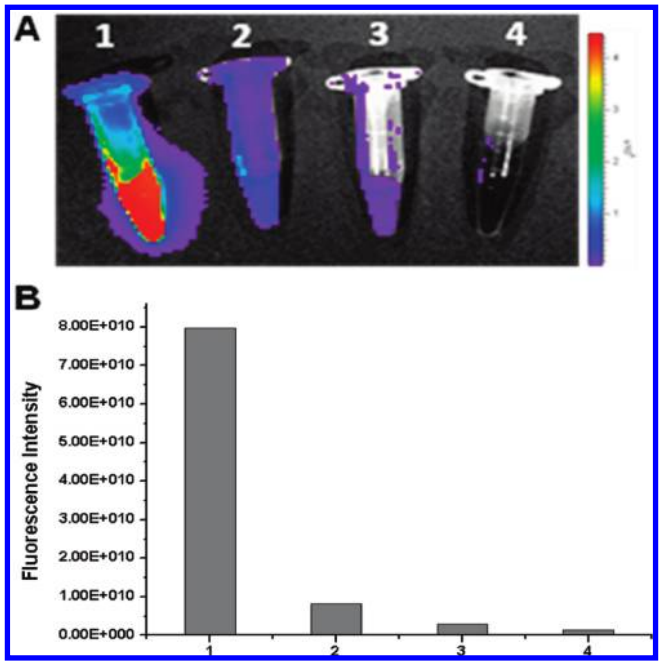

Figure 3. (A) The fluorescence of microtubes containing PS DNA25-Cy5.5 singlet in PBS before (1) and after hybridizing with the complementary PO DNA22-BHQ3 singlet at the molar ratios of 1:1 (2), 1:10 (3) and 1:50 (4). (B) Fluorescence quantitation using Living Image 2.5 software.

the fluorescence intensity decreased by about 90% while the decrease is essentially 100% at the 1:50 molar ratio. These results illustrate the efficient fluorescent quenching exhibited by these duplexes.

Three SKH-1 normal mice in each group were imaged 10 min after intravenous administration of 1 nmol of PS DNA25-Cy5.5 singlet or the PS DNA25-Cy5.5/PO cDNA22-BHQ3 duplex prepared at either a 1:1, 1:10 or 1:50 molar ratio. Mice received only PBS as control. The images presented in Figure 4A are representative and show obvious increasing effects of duplex quenching and lower background with the administration of increasing dosage of the free inhibitor minor strand DNA BHQ3-PO22. As shown in Figure 4B, the fluorescence background was eventually reduced to insignificance ($P > 0.05$, compared with PBS). In Figure 4C, the quenching efficiency is about 44%, 67% and 82% for mice receiving the PS DNA25-Cy5.5/PO cDNA22-BHQ3 duplex at molar ratios of 1:1, 1:10 and 1:50 respectively.

Target Binding in Vitro. To provide evidence that the PS DNA25-Cy5.5/PO cDNA22-BHQ3 duplex is still capable of dissociating at its mRNA target by an antisense mechanism despite a 22 mer minor strand compared to the 18 mer minor strand used previously,[1] the anti mdr1 duplex was incubated at increasing concentrations in KB-G2 (mdr1++) cells and in control KB-31 (mdr1+/−) cells at 37 °C for 3 h and the fluorescent intensity measured in 96-well plates as before. The results are shown in Figure 5. While the fluorescence intensity of KB-31 cells did not change appreciably with concentration, the fluorescence in the KB-G2 increased linearly with duplex concentration and became significantly higher than KB-31 signal at all concentration greater than 100 nM, providing evidence for an antisense mechanism by specific mRNA binding.

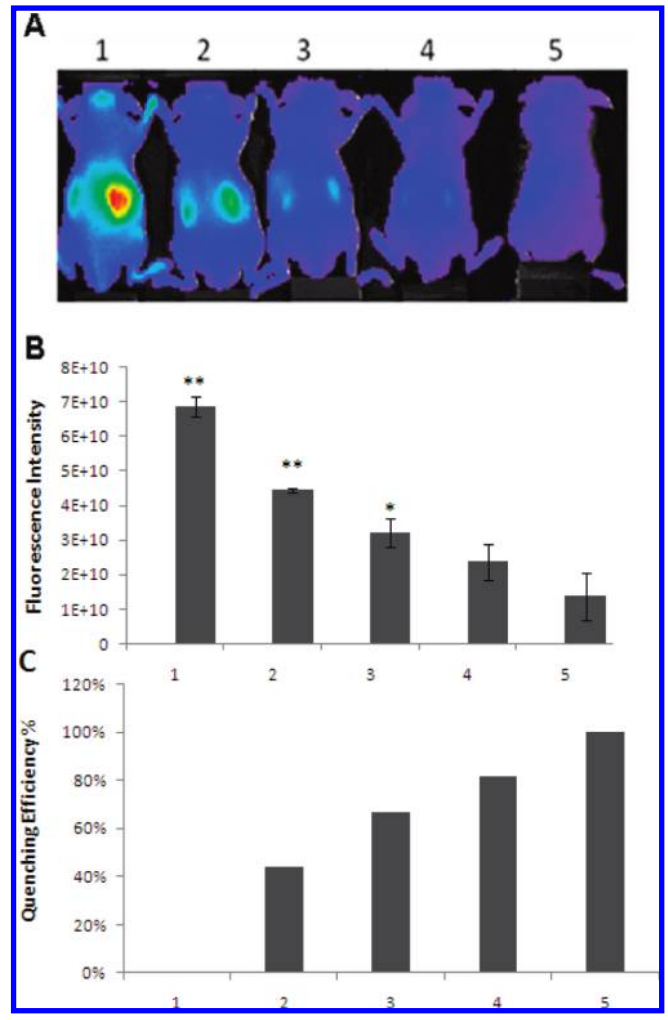

Figure 4. (A) Whole-body fluorescence images in the dorsal view of SKH-1 mice at 10 min post intravenous injection of 1 nmol of PS DNA25-Cy5.5 singlet (1) or the PS DNA25-Cy5.5/PO cDNA22-BHQ3 duplex prepared at molar ratios of 1:1 (2), 1:10 (3) or 1:50 molar ratio (4). Animals received PBS as control (5). (B) Histograms representing the average whole-body fluorescence intensity for animals grouped as in A; error bars represent one standard deviation for three replicates. (**, $P < 0.01$; *, $P < 0.05$ compared to PBS mice). (C) Histograms representing the quenching efficiency (see text) for animals grouped as in A. Results are presented as the percent compared to the PBS animals set initially at 0%.

Target Binding in Vivo. Nude male mice each bearing KB-G2 tumors in the left thigh received an intravenous injection of 1 nmol of the PS DNA25-Cy5.5/PO cDNA22-BHQ3 duplex prepared at a 1:10 molar ratio and were imaged 1 h postinjection. The minimal improvement in quenching efficiency shown in Figure 4 for the duplex administered at a 1:50 compared to a 1:10 molar ratio was not considered

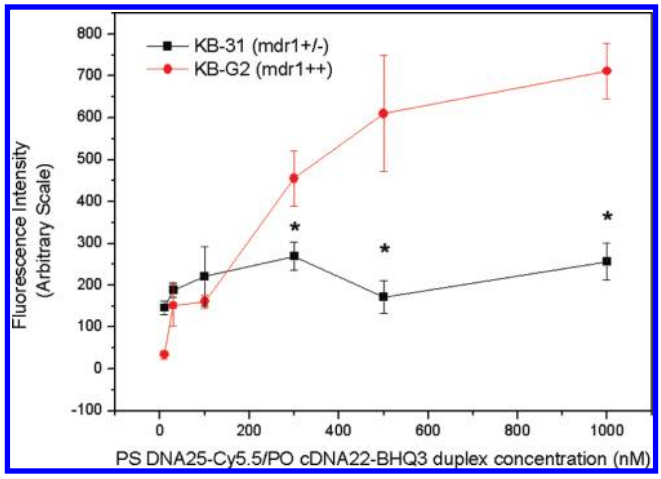

Figure 5. Cellular fluorescence of KB-G2 (mdr1++) and KB-31(mdr1+/−) cells after incubation for 3 h with the anti-mdr1 duplex (PS DNA25-Cy5.5/PO cDNA22-BHQ3) as a function of duplex concentration. Error bars represent standard deviations for four replicates. (*, $P < 0.05$.)

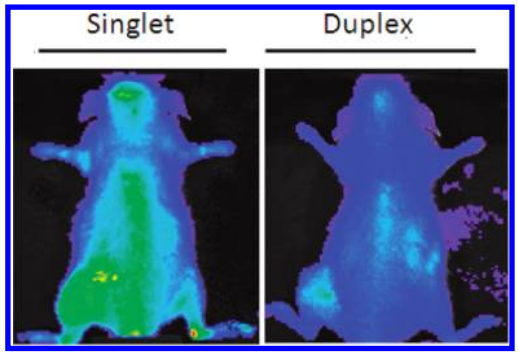

Figure 6. Whole-body dorsal fluorescence images of mice bearing a KB-G2 tumor in the left thigh at 1 h postintravenous injection of 1 nmol of the PS DNA25-Cy5.5 singlet or the PS DNA25-Cy5.5/PO cDNA22-BHQ3 duplex at a 1:10 molar ratio.

sufficient to justify administering excessive minor strand that may influence dissociation in the tumor. As shown in Figure 6, the extensive whole body fluorescence in the animal receiving the singlet, made tumor accumulation difficult to appreciate. By contrast, the whole body fluorescence of animals receiving the duplex is much lower and the tumor is much more evident. The obvious tumor fluorescence provides evidence of mRNA antisense targeting in vivo.

Discussion

When a fluorescent antisense DNA singlet is used to image tumor in vivo, the fluorescence background in nontarget tissues can mask the signal and lead to low target-to-background ratios and limit sensitivity as is evident from Figure 6. The overall objective of this research is to design fluorophore/inhibitor DNA duplexes to target mRNAs in tumor by an antisense mechanism and with background fluorescence reduced to insignificance. While we have previously shown impressive tumor images in mice using our standard PS DNA25-Cy5.5/PO cDNA18-BHQ3 duplex,[1,2] our goal of eliminating background fluorescence has not yet been achieved.

Prior to this investigation, we consider that kidney fluorescence could be eliminated by preventing the duplex from clearing through the kidneys. In a published study, the duplex was attached to streptavidin, a 60 kDa protein, via a stable biotin bond in the manner that our studies of streptavidin nanoparticles for Auger electron radiotherapy of cancer are proceeding.[17] The anti-mdr1 Cy5.5-PS DNA25/BHQ3-PO cDNA10/streptavidin nanoparticle was administered to KB-G2 tumor bearing mice. As shown in Figure S1 in the Supporting Information, tumor accumulation was prominent in all images. However, compared to the tumored animal receiving the streptavidin-bound duplex, the animal receiving the streptavidin-free duplex provided a more positive tumor-to-background ratio, except in kidneys. Obviously the addition of streptavidin accomplished the goal of restricting fluorescence in the kidneys but at the expense of increased fluorescence in circulation and in other organs. Apparently dissociation was still occurring as before but the Cy5.5-DNA25, when tethered to streptavidin, may be unable to clear through the kidneys and remains in circulation.

We earlier reported that fluorescence background was not observed when, as a control, the fluorophores were reversed and the Cy5.5 fluorophore was attached to the PO DNA minor rather than the major strand.[1] Subsequent studies confirmed that when on a PO DNA singlet, the Cy5.5 fluorophore is rapidly released from its DNA almost certainly by endonuclease attack on this oligomer and is therefore free to be cleared from the whole body to provide, after a time, a minimal background fluorescence. However, if the Cy5.5 is on a PS DNA singlet, because of the stability of this oligomer to nucleases, this singlet will clear more slowly from circulation and will accumulate in kidneys along with its label. Therefore in the hope of achieving nuclease stability by blocking both ends of the PO DNA chain and in a second study, we engineered an anti-mdr1 Cy5.5-PO10 PS15/BHQ3-PS10 duplex in which the anti-mdr1 antisense sequence was again a 25 mer but now with the first 10 bases as a Cy5.5-PO rather than Cy5.5-PS DNA and hybridized with a 10 mer PS BHQ3-DNA. Finally to complete the 25 mer length to the antisense DNA, the 10 mer PO (lower case) was elongated with a 15 mer PS (upper case) DNA:

Cy5.5-linker-cct-cgc-gct-c-CA-GCC-CTA-CCT-ACA-A-5′

BHQ3-linker-GGA-GCG-CGA-G-3′

In this manner, it was expected that duplex dissociation at its mRNA target would be unchanged but dissociation elsewhere with release of the fluorescent Cy5.5-PO10PS15 would be vulnerable to nucleases and lead to release of the free Cy5.5 fluorophore and rapid clearance through the kidneys. In support of this hypothesis, the whole body fluorescence in both normal and tumored animals did decrease more rapidly following administration of the new Cy5.5-PO10PS15/BHQ3-PS10 duplex compared to the pre-

vious Cy5.5-PS25/BHQ3-PO10 duplex and the images showed an obvious improvement in background, presumably because of nuclease attack on the singlet PO DNA attaching the Cy5.5. However, although the tumor/normal thigh fluorescence ratio also showed improvement at all time points over 24 h, the absolute tumor fluorescence decreased along with the whole body fluorescence. When tissues were imaged, ex vivo, a lower fluorescence was evident in almost all tissues sampled with the exception of stomach, but unfortunately including the tumor. We concluded that nuclease attack on the 10 mer PO DNA to which the Cy5.5 was attached was responsible for the favorable rapid clearance of background fluorescence but also responsible for the unfavorable rapid clearance within the tumor. We therefore concluded that duplexes in which the fluorophore on the major strand is attached to a PO DNA did not deserve further consideration.

In this present study, we used a homogenate assay to help identify the source of duplex dissociation in normal tissues that must be occurring by some mechanism to explain the fluorescence background within the animal and developed methods to minimize it. The results presented in Figure 1 provide evidence that liver was mainly responsible for the duplex dissociation providing this background fluorescence. Thereafter gel electrophoresis was used to analyze liver homogenates into which five different duplexes were incubated. As shown in Figure 2, this homogenate assay confirmed the expected increase in stability with increasing length of the minor strand and showed that the PS25/PO22 duplex was the most stable to the liver homogenate incubation. Using this duplex (i.e., PS DNA25-Cy5.5/PO cDNA22-BHQ3) we have shown in Figure 4 that the whole body fluorescence can be reduced to insignificance if the duplex is coadministered with at least a 10-fold molar excess of the minor strand. Presumably some limited degree of dissociation of the duplex is occurring in vivo despite the longer minor strand and that the presence of excess minor strand is required to drive the equilibrium back toward duplex formation. Nevertheless, the coadministration of a fluorophore/inhibitor duplex along with an excess of the inhibitor minor strand should be practical in clinical applications.

While the PS DNA25-Cy5.5/PO cDNA22-BHQ3 duplex has been shown to provide the required stability in vivo, the remaining question is whether this duplex is still capable of dissociation in its target. Fortunately, as shown in Figures 5 and 6, both in vitro and in vivo, evidence of mRNA antisense targeting of the anti-mdr1 duplex was obtained. In subsequent studies, we hope to investigate the effect of elongating the major strand while keeping the minor strand at 22 mer to determine whether the dissociation of the new duplex in its tumor target can be improved while maintaining insignificant background fluorescence.

Conclusion

In summary, the work presented here has demonstrated that liver was likely to be the major source within the normal tissues responsible for the duplex dissociation providing the unwanted fluorescence background. Combining gel electrophoresis and liver homogenates allowed us to demonstrate the increasing stability with increasing length of the minor strand of the duplex. The result was a fluorophore/inhibitor DNA duplex that reduced background fluorescence to insignificance and, at the same time, target its mRNA in cells and in tumor bearing animals.

Supporting Information Available: Details of experiments in eliminating the kidney fluorescence background. This material is available free of charge via the Internet at http://pubs.acs.org.

MP100229Z